Directed rotational motion of birefringent particles by randomly changing the barrier height at the threshold in a washboard potential

Basudev Roy* and Erik Schäffer

Centre for Plant Molecular Biology, University of Tübingen, Tübingen 72076, Germany

This communication presents a simulation study of the directed rotational motion of a birefringent spherical particle trapped in optical tweezers with randomly varying ellipticity of a trapping light at the point of threshold. When noise is not applied, the potential barrier due to the linear component of the polarization is simulated to be sufficient to prevent directed rotation till a certain threshold value of ellipticity. Random variations to the ellipticity cause random variations in the barrier height, including instants when the barrier is lower than the threshold energy level. It is due to this that the particle exhibits directed rotational motion at ellipticity lower than the threshold value. We also examine the rotational velocity of the birefringent particle as a function of the extent of zero-mean random noise applied to the ellipticity.

Keywords: Birefringent particles, barrier height rotational motion, washboard potential.

A tilted washboard potential is known to facilitate giant enhancement of diffusive behaviour[1]. It is particularly relevant in biological systems like motion of motor proteins in cytoskeletal meshwork, which can be described as a thermally forced ratchet. Such tilted washboard potentials have also been observed in systems with rotational motion[2], translational motion[3–5] and elsewhere[6,7]. As shown by Tatarkova *et al.*[3], when the tilt in potential exceeds a certain threshold, it establishes a stable running mode that accumulates particles towards the lowest well showing a directed steady motion. In these systems, height of the washboard potential, sometimes varying spatially, may still be held constant in time.

An interesting situation emerges where the potential height is not static but continuously changing in time, albeit randomly, between values which are sometimes higher than the threshold and sometimes lower. A particle may escape above one potential barrier under the influence of thermal noise at some given point of time but may not overcome the next, being higher. We ask the question whether a stable running mode can still be established in such cases and under what conditions. In order to create such a time-varying array of potential barriers, a rotational system was chosen.

*For correspondence. (e-mail: basudev.roy@uni-tuebingen.de)

Rotation of particles trapped in optical tweezers has been demonstrated by turning the axis of linear polarization[2], applying circularly polarized light[8], an extra rotating electric[9] or magnetic field[10] and even trapping an asymmetric particle at two locations while moving one of the spots[11]. In most of these cases, the dipole moment of the particle, either the intrinsic or the induced, interacts with the field. Spontaneous rotation of a birefringent particle in a single-beam optical tweezer uses interaction between the induced dipole moment of the particle and the electric field. The torque applied due to an elliptically polarized trapping light is given as[8]

$$\tau = -\frac{\varepsilon}{2\omega} E_0^2 [D\sin(2\theta) - E], \tag{1}$$

$$D = \sin(kd(n_0 - n_e))\cos(2\phi), \tag{2}$$

$$E = (1 - \cos(kd(n_0 - n_e)))\sin(2\phi). \tag{3}$$

Here ω is the frequency of light, E_0 the electric field, ε the permittivity, k the wavevector of light, d the diameter of the particle, $n_0 - n_e$ the birefringence of the particle, θ the angle between the linear component of light and the ordinary direction of the refractive index of particle, and $\tan(\phi)$ is the ellipticity of light.

This torque has two components, one orienting the optic axis of the particle towards the major axis of ellipticity, and the other generating continuous rotation of the particle as indicated by the first and the second terms on RHS of eq. (1) respectively. The effective potential due to this torque becomes a washboard potential in which the
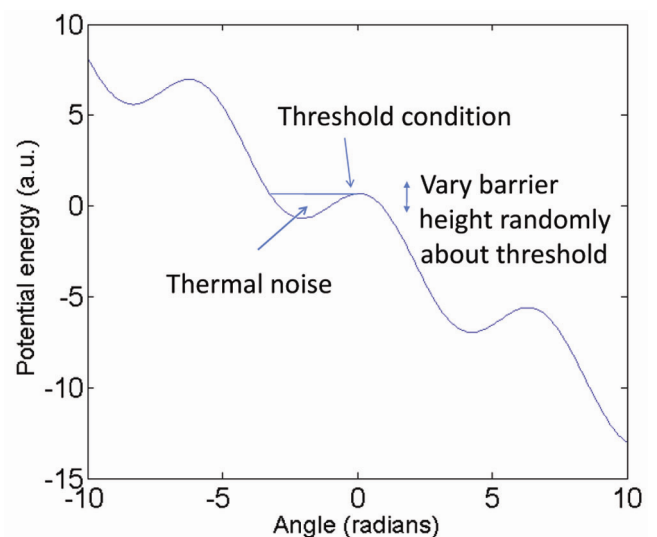

Figure 1. Plot indicating washboard potential when the thermal noise raises the energy enough to equal the barrier height. This is the threshold condition. When the barrier height is randomly changed with the mean at the threshold, or the washboard tilted, it leads to directed rotational motion.

particle diffusively rotates. The height of the potential barrier and the corresponding tilt can be controlled by the degree of ellipticity of the trapping light. This problem becomes similar to the case when the axis of the linearly polarized trapping light is rotated physically, till a certain value of rotation rate of the polarization vector, to generate an extra torque[2]. This 'maximum torque'[2] depends upon the extent of angular momentum transferred to the particle, thereby dependent upon the intensity of the laser beam used and the scattering efficiency of the particle. There is a situation while using the elliptically polarized light that the height of the potential barrier is barely enough to obstruct steady rotational motion due to the circular component. Increase in temperature of the system or lowering of the potential barrier results in continuous rotation. The onset of continuous rotation due to increase in temperature has been reported in the literature[12]. The present communication explores similar onset of continuous rotation by randomly varying the height of the potential barrier upon rapidly changing the ellipticity of the trapping light at the threshold (Figure 1).

The equation governing the rotational dynamics of the particle is

$$v\frac{d\theta}{dt} = \varepsilon_1\tau + (2k_BTv)^{1/2}\eta(t). \tag{4}$$

The equation that governs the rotational dynamics of the particle is essentially the rotational Langevin equation with the extra torque τ due to the light described by eq. (1). The factor ε_1 gives the efficiency of the trapping system dependent on the fraction of trapping light interacting with the particle. This strongly depends upon particle size and wavelength of the trapping light. $\eta(t)$ indicates a Gaussian-distributed random noise centred about 0. v is the rotational drag coefficient, k_B the Boltzmann constant, T the temperature of the system and t is the time. Equation (4) can be written as

$$v\frac{d\theta}{dt} = -A\cos(2\phi)\sin(2\theta) + B\sin(2\phi) + (2k_BTv)^{1/2}\eta(t). \tag{5}$$

The coefficients A and B indicate parameters shown in eq. (1). When the angle ϕ in eq. (5) is equal to 0, the second term on the right-hand side vanishes and only a sinusoidal potential is left behind corresponding to a linearly polarized light. Further, when this ellipticity angle ϕ is $\pi/4$, the first term vanishes indicating a completely circularly polarized light when the particle rotates, let us say at Ω. There is also an angle ϕ_T at which the system can trickle past the sinusoidal potential and barely starts rotating. Thus we get the two conditions

$$v\Omega = B + (2k_BTv)^{1/2}\eta(t), \tag{6}$$

$$0 = -A\cos(2\phi_T)\sin(2\theta) + B\sin(2\phi_T) + (2k_BTv)^{1/2}\eta(t). \tag{7}$$

The threshold condition can be calculated from eqs (6) and (7) to yield the result

$$\cot\left(\frac{kd(n_0-n_e)}{2}\right) = \frac{\frac{(2k_BTv)^{1/2}}{v\Omega} + \sin(2\phi_T)}{\cos(2\phi_T)}. \tag{8}$$

Equation (8) can be used to accurately determine the birefringence of the particle upon accounting for thermal noise. The maximum rotational rate should show up in the power spectrum as a Gaussian-distributed line. The first term in the numerator of the right-hand side of eq. (8) is essentially the ratio of the width of this Gaussian to the centre of the maximum rotation rate line at circular polarization. In principle, the thermal noise should affect the way rotational rate responds to change in ellipticity. It has been demonstrated that the conventional technique without accounting for noise, given in Juodkazis et al.[13], is accurate to 5%. This correction has the potential to provide more accurate measurement of birefringence. The presence of the Gaussian random noise in eq. (6) is also the reason why a steady rotation cannot be recorded when the value of the standard deviation of random noise, given in the second term of the equation, is larger than B. The error in detection of the rotation rate would be higher than the magnitude of the rate itself. Hence, weak values of birefringence would not be able to generate steady rotation.

The angle ϕ_T in eq. (7) is the parameter which allows control over the potential barrier. This can yield the value of birefringence to high accuracy. When ϕ_T is randomly changed keeping the mean at the level corresponding to the threshold, the particle would indeed exhibit continuous rotational motion for half the cycle when the barrier is lower than the mean.

We have solved eq. (9) to ascertain the angular coordinate of the particle as a function of time and then taken the Fourier transform (FT) of the derivative of the time series to ascertain directed motion

$$\frac{d\theta}{dt} = -\frac{A}{v}\cos(C)\sin(\theta/2) + \frac{B}{v}\sin(C) + \left(\frac{2k_BT}{v}\right)^{1/2}\eta(t), \tag{9}$$

$$C = 2\phi(1 + \alpha W(t)). \tag{10}$$

$W(t)$ is a time-varying random Gaussian noise with a mean of 0 and a standard deviation of 2, which has been scaled by a parameter α to vary the extent of noise. We have used $(A/v) = 1$, $(B/v) = 0.2$ and $(2k_BT/v)^{1/2} = 0.4$. This kind of a system can be generated in an optical

tweezer with the degree of ellipticity of the trapping light being changed randomly about a mean value. However, the experimental system has to have the ellipticity change fast enough (faster than v/A) to make the process truly random.

Equation (9) can be simplified into the form

$$\frac{d\theta}{dt} = -\frac{\delta V(\alpha, \theta)}{\delta \theta} + 0.4\eta(t). \tag{11}$$

A directed continuous rotation is demonstrated in Figure 2 using a Gaussian-distributed random noise with $\pm 20°$ extent in ϕ indicated by the upper curve. The thermal noise merely modifies the threshold potential. The lower curve in Figure 2 exhibits random motion across barriers (Kramers transitions) due to thermal noise which is observed as a step-like behaviour in the FT of the angular velocity, which is however not a steady directed motion. The extra peak in the upper curve in Figure 2 indicates directed motion which is not present in the lower curve.

We perform another study to understand how the noise affects the probability of directed rotational motion. The probability that a particular level of potential energy is populated is given by the Maxwell–Boltzmann law, namely

$$P = \exp(-V(\alpha, \theta)), \tag{12}$$

where $V(\alpha, \theta)$ is the potential energy at the angular coordinate θ with an added random perturbative noise to the barrier height, ζ_1 by changing α. In this equation, the temperature has been assumed to be such that $k_B T = 1$. Then the probability that the noise applied would induce directed angular motion can be calculated from eq. (13)

$$Q(\alpha, \theta) = [\exp(-V(0, \theta)) - \exp(-V(\alpha, \theta))]. \tag{13}$$

In the calculation of Q, only the non-negative values were used since a negative value would indicate that $V(0, \theta)$, which is the maximum value of the thermal noise of the system at threshold, is lower than the instantaneous potential. The negative values of Q are unphysical because a classical particle with a certain energy cannot move past a higher potential barrier. We assume that there is no tunnelling motion through the barrier while obeying classical physics.

A histogram of Q for a particular value of α, which serves to lower the potential barrier, reveal the preferred value of angular velocity. This is where a maximum probability of directed rotational motion appears. Figure 3 shows a typical histogram for a noise amplitude α of 0.5.

The peak velocity of directed rotational motion can be expected to increase as the width of the distribution of random noise is increased. This has been plotted in Figure 4. The dependence of velocity on the width of

noise distribution is linear. Further, as indicated by the intercept of the fitted straight line, when there is no extra noise at the threshold, there is no directed angular motion when the peak angular velocity is 0.
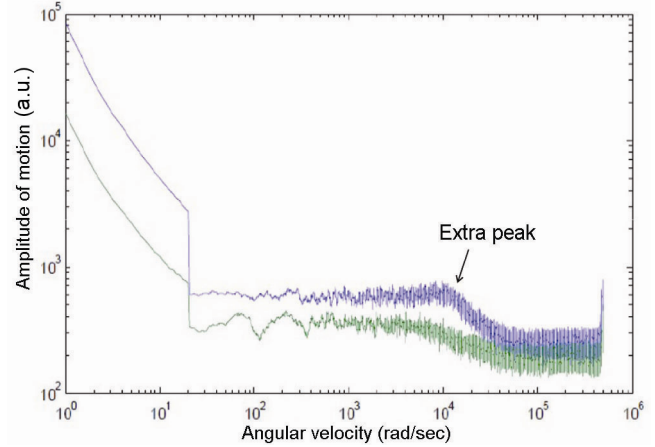

Figure 2. Plot (the lower curve without the extra peak) indicating Fourier transform (FT) of the angular coordinate obtained by numerically solving eq. (5) when the ellipticity of the quarter-wave plate has held constant at the threshold angle $2\phi = 22°$. The upper curve with the extra peak indicates FT of the angular coordinate in the presence of an added Gaussian distributed random noise on the ellipticity angle of $22° \pm 20°$. The extra peak in the blue curve indicates continuous rotation upon addition of Gaussian distributed random noise. The (the lower curve without the extra peak) exhibits random motion across barriers (Kramers transitions) due to thermal noise observed in the FT of the angular velocity.
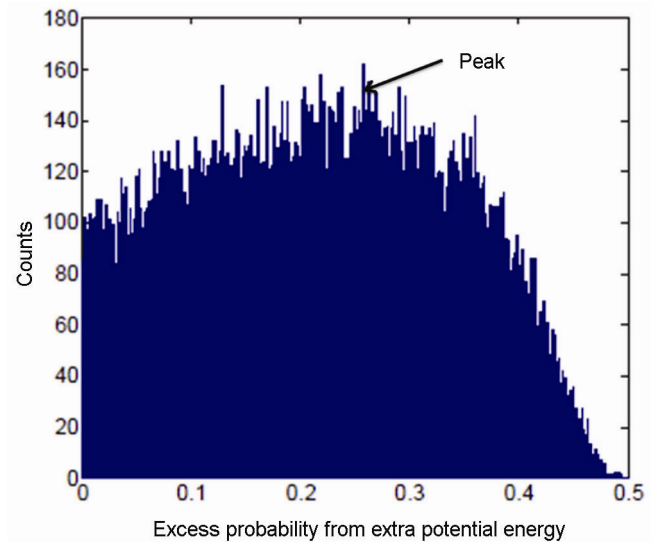

Figure 3. Histogram indicating the frequency with which a certain value of excess potential appears. The x-axis indicates the Maxwell–Boltzmann probability at a certain value of potential energy in the presence of thermal noise (Q in eq. (13)) while the y-axis indicates the frequency with which it appears. The potential barrier preventing directed motion is modulated with a zero-mean Gaussian-distributed random noise and the corresponding distribution of potential energies ascertained. There is a maximum value of the excess energy which would in turn indicate the most probable velocity of the particle. The amplitude of noise α is 0.1. A total of 200,000 barrier energy values were considered.
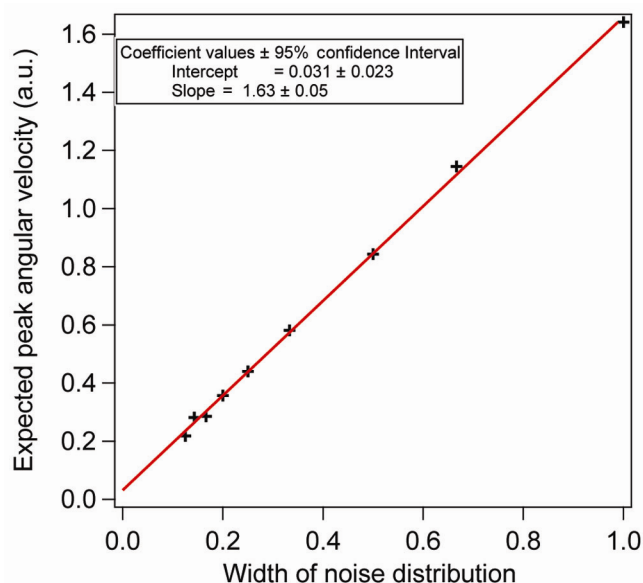
Figure 4. Plot indicating the expected peak angular velocity of particle as a function of width of the zero-mean Gaussian random noise α applied to the height of the potential barrier. The velocity is estimated as proportional to the square root of $(V(\alpha, \theta) - V(0, \theta))$, which is obtained using the peak of the histogram (like Figure 3) and substituting it in eq. (13). The angular velocity is linearly proportional to the width of the Gaussian noise.

This experiment can be used to ascertain the birefringence of small spherical particles of the dimension of a few micrometres accurately. The thermal noise complicates the method of detection of birefringence reported in Juodkazis *et al.*[13], which is only accurate to about 5%. A more accurate measurement would require accounting for the thermal random noise.

This communication described a new way of generating the washboard potential and producing directed continuous motion upon changing the barrier height randomly at the threshold. It also analysed, in two different ways, the velocity of the directed motion under specific amounts of random noise.

1. Reimann, P., Van den Broeck, C., Linke, H., Hanggi, P., Rubi, J. M. and Perez-Madrid, A., Giant acceleration of free diffusion by use of tilted periodic potentials. *Phys. Rev. Lett.*, 2001, **87**, 010602.
2. Pedaci, F., Huang, Z., van Oene, M., Barland, S. and Dekkar, N. H., Excitable particles in an optical torque wrench. *Nat. Phys.*, 2011, **7**, 259–264.
3. Tatarkova, S. A., Sibbett, W. and Dholakia, K., Brownian particle in an optical potential of the washboard type. *Phys. Rev. Lett.*, 2003, **91**, 038101.
4. Faucheux, L. P., Bourdieu, L. S., Kaplan, P. D. and Libchaber, A. J., Optical thermal ratchet. *Phys. Rev. Lett.*, 1995, **74**, 1504.
5. Sanchez-Palencia, L., Carminati, F.-R., Schiavoni, M., Renzoni, F. and Grynberg, G., Brillouin propagation modes in optical lattices: interpretation in terms of nonconventional stochastic resonance. *Phys. Rev. Lett.*, 2002, **88**, 133903.
6. Devoret, M. H., Martinis, J. M., Esteve, D. and Clarke, J., Resonant activation from the zero-voltage state of a current-biased Josephson junction. *Phys. Rev. Lett.*, 1984, **53**, 1260.
7. Chen, Y.-C. and Lebowitz, J. L., Quantum particle in a washboard potential. II. Nonlinear mobility and the Josephson junction. *Phys. Rev. B*, 1992, **46**, 10751–10762.
8. Freise, M. E. J., Nieminen, T. A., Heckenberg, N. R. and Rubinsztein-Dunlop, H., Optical alignment and spinning of laser-trapped microscopic particles. *Nature*, 1998, **394**, 348–350.
9. Rowe, A. D., Leake, M. C., Morgan, H. and Berry, R. M., Rapid rotation of micron and submicron dielectric particles measured using optical tweezers. *J. Mod. Opt.*, 2003, **50**, 1539–1551.
10. Gosse, C. and Croquette, V., Magnetic tweezers: micromanipulation and force measurement at the molecular level. *Biophys. J.*, 2002, **82**, 3314–3329.
11. Roy, B., Bera, S. K. and Banerjee, A., Simultaneous detection of rotational and translational motion in optical tweezers by measurement of backscattered intensity. *Opt. Lett.*, 2014, **39**, 3316–3319.
12. Casado, J. M., Coherence resonance in a washboard potential. *Phys. Lett. A*, 2001, **291**, 82–86.
13. Juodkazis, S., Matsuo, S., Murazawa, N., Hasegawa, I. and Misawa, H., High-efficiency optical transfer of torque to a nematic liquid crystal droplet. *Appl. Phys. Lett.*, 2003, **82**, 4657–4659.

Greener production of magnetic nanoparticles and their fabrication

Ashima Sharma and Kavita Tapadia*

Department of Chemistry, National Institute of Technology, Raipur 492 010, India

In the present study green synthesis of magnetic nanoparticles has been described. Green tea was used in the synthesis of these nanoparticles due to its reducing property. The surface of green tea–magnetic nanoparticles was modified with tetra ethyl orthosilicate for silica coating, and further silica-coated green tea–magnetic nanoparticles were amine-activated by (3-aminopropyl)triethoxysilane. The proposed work is simple and cost-effective. Characterization of the structure and composition of green synthesized magnetic nanoparticles was formulated by X-ray diffraction analysis, Fourier transform-infra red, scanning electron microscope, electron dispersive X-ray and high-resolution transmission electron microscope.

Keywords: Amine activation, fabrication, green synthesis, green tea, magnetic nanoparticles.

*For correspondence. (e-mail: ktapadia.chy@nitrr.ac.in)